Liquid immiscibility and the origin of alkali-poor carbonatites

B. A. KJARSGAARD AND D. L. HAMILTON

Department of Geology, The University, Manchester M13 9PL

Abstract

The work on liquid immiscibility in carbonate-silicate systems of Freestone and Hamilton (1980) has been extended to include alkali-poor and alkali-free compositions. Immiscibility is shown to occur on the joins albite-calcite and anorthite-calcite at 5 kbar. These results make it possible to interpret ocellar structure between calcite-rich spheroids in lamproite or kimberlite host rock as products of liquid immiscibility. The common sequence of rock types found in carbonatite complexes of melilitite-ijolite-urtite-phonolite is interpreted as being the result of both fractional crystallization and liquid fractionation, the corresponding carbonatite composition changing from nearly pure $CaCO_3$ ($\pm MgCO_3$) progressively to natrocarbonate. A carbonate melt cooling in isolation will suffer crystal fractionation, the residual liquid producing the rarer ferrocarbonatites, etc., whilst the crystal accumulate of calcite (dolomite) plus other phases such as magnetite, apatite, baryte, pyrochlore, etc., are the raw material for the coarse-grained intrusive carbonatites commonly found in ring complexes.

KEYWORDS: carbonatites, liquid immiscibility, carbonate-silicate systems.

Introduction

THE genesis of carbonatites and associated alkaline rocks remains a controversial geological topic. Three widely different models have been proposed suggesting that carbonatite magmas are: (1) a direct product of partial melting of mantle material (von Eckermann, 1948; Holmes, 1952; Dawson, 1962, 1966; Eggler, 1975; Koster Van Groos, 1975); (2) a differentiation product of a carbonated silicate liquid (King, 1949; King and Sutherland, 1960; Watkinson and Wyllie, 1971; Wyllie, 1987); (3) an immiscible carbonate liquid separated from an originally homogeneous carbonated silicate melt (von Eckermann, 1961; King, 1965; Koster Van Groos and Wyllie, 1966, 1968, 1973; Middlemost, 1974; Cooper *et al.*, 1975; Le Bas, 1977, 1981; Freestone and Hamilton, 1980).

The hypothesis of liquid immiscibility has recently been favoured by many authors, but a major objection is the contrasting evidence deduced from field and experimental relations. While conclusive experimental work on silicate-carbonate immiscibility has been performed for alkali-rich conditions (Koster van Groos and Wyllie, 1966, 1968, 1973; Verwoerd, 1978; Wendlandt and Harrison, 1979; Freestone and Hamilton, 1980), research on alkali-poor systems has not revealed a two-liquid field (Watkinson and Wyllie, 1969, 1971). Other experimental studies under alkali-poor conditions have produced ambiguous results, usually causing the authors to reject the existence of a stable two-liquid field (Brey, 1977; Bedson, 1983). In contrast, field relations reveal the majority of carbonatites (with the exception of the rare natrocarbonatites) to be alkali-poor or free, generally calcitic or dolomitic (Le Bas, 1977, 1981) and therefore an origin by immiscibility is usually ruled out.

Thus petrologists who favour the hypothesis of liquid immiscibility for carbonatites start with an alkali-rich carbonatite magma which must lose alkalis so that the magma evolves to an alkali-poor carbonatite. Transport by fenitizing fluids (Le Bas, 1981; Woolley, 1982) or meteoric waters are usually invoked as the mechanism to produce this alkali loss. Le Bas (1981) considers one of the hallmarks of a 'true' carbonatite is the intense alkali metasomatism (fenitization) bordering carbonatite intrusions. However geological literature contains descriptions of localities where the field relations reveal apparent immiscibility textures between alkali-poor carbonates and silicates with no associated fenites. Examples of this type appear to be

Mineralogical Magazine, March 1988, Vol. 52, pp. 43-55

restricted to basic alkalic rocks, e.g. spheres of calcite or dolomite in a melilite basalt (von Eckermann, 1961, 1966), in kimberlite (Dawson and Hawthorne, 1973), in a lamprophyre (Ferguson and Currie, 1971) and in dolerite (Bogoch and Magaritz, 1983).

In this paper we report the results of an experimental investigation on the extent of silicate–carbonate liquid immiscibility in the synthetic system SiO_2–Al_2O_3–Na_2O–CaO–CO_2. Freestone and Hamilton (1980), on the basis of their research at alkali-rich conditions, constructed a two-liquid field which they assumed closed toward CaO-rich compositions. This assumption was based on the previously published work of Watkinson and Wyllie (1971) and Brey (1977); none of these authors detected liquid immiscibility in alkali-poor conditions. The present study, however, has proved the existence of a large two-liquid field which includes alkali-free liquids, i.e. the two-liquid field extends to the alkali-free side of the pseudoternary triangle of Freestone and Hamilton (1980).

Experimental methods

Starting materials. Four silicate glasses, the compositions of which are shown in Table 1, were used. The albite glass was kindly provided by Pilkington Brothers Plc. Glasses of anorthite and compositions E1 and E2 were prepared by multiple fusions of oxide mixes and analysed on a Cameca microprobe. The carbonates used were analytical grade $CaCO_3$ and Na_2CO_3 which were stored at 110 °C to keep dry. The majority of runs had mechanical mixes of glass plus carbonate which were weighed out, thoroughly hand ground in an agate mortar and redried before sealing in $Ag_{40}Pd_{60}$ tubes of dimensions 0.2 inches OD × 1.25 inches long. About 0.5 g of sample fitted easily into these tubes. This silver/palladium alloy was chosen because its greater strength compared with platinum was required to contain the CO_2 when the pressure was released at the end of the run. In some cases up to 10% of silver oxalate or oxalic acid dihydrate was added to the sample tubes; the first was found to have little effect on the run products whereas the latter had a large, and to date largely unfathomed, effect on the run products and is worthy of further study.

Experiments. Sample charges were run in an internally heated, argon medium-pressure vessel. Temperature, believed accurate to ±5 °C, was measured using $Pt/PtRh_{13}$ thermocouples. Two thermocouples were employed, one at each end of the sample holder; small temperature gradients were eliminated by slightly tilting the pressure vessel. Pressure was measured using a manganin cell which had been previously calibrated against a Heise gauge which is used only for calibration purposes. Run duration varied from 3 to 26 hours. Samples were quenched by turning off the furnace power while simultaneously tilting the pressure vessel through 90° so that the hot gas surrounding the samples was displaced by cold gas. The first 200 °C drop in temperature occurs in *c.* 10 seconds at constant pressure.

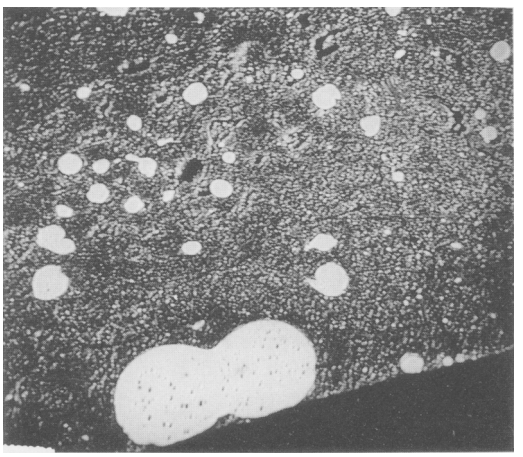

FIG. 1. Back-scattered electron image (BSE). Run KH 58, $Ab_{50}NC_{50}$ at 5 kbar and 1250 °C. Shows numerous silicate droplets in sodium carbonate host. Diameter of large coalescing spheres is about 500 μm.

Run products consisted of 1 or 2 quenched liquids, depending on starting bulk composition. Two runs with added oxalic acid contained tabular 0.2–0.5 mm long gehlenite crystals in addition to two quenched liquids. Silicates quenched to glasses varying from transparent colourless through very light translucent pale yellow in colour to opaque. Carbonates quenched to friable, translucent fine-grained aggregates. Ca-rich and Na-rich carbonate melts quenched to structureless aggregates (Fig. 1), while carbonate melts with compositions intermediate to this quenched to dendritic intergrowths of calcite and nyerereite (Fig. 2*a*, *b*).

Table 1 Starting Materials

	SiO_2	Al_2O_3	Na_2O	CaO	MgO	Total
Albite	68.43	18.74	11.54	0.01	-	98.72
Anorthite	44.59	35.21	-	19.85	-	99.65
E1	63.99	13.94	-	23.17	-	101.10
E2	41.00	22.12	-	33.63	3.02	99.77

Table 2 Run Data

Run No.	Composition (wt %)	Added Components (wt %)	P (kb)	T (°C)	Time (h)	Assemblage
KH 9	$Ab_{50}CC_{50}$	10% S.O.	4.9	1250	3	L_S + V
KH 10	$Ab_{38}CC_{62}$	10% S.O.	4.9	1250	3	L_S + L_C + V
KH 11	$Ab_{25}CC_{75}$	10% S.O.	4.9	1250	3	L_S + L_C + V
KH 16	$Ab_{75}CC_{25}$	14.41% N.C.	5.0	1250	4	L_S + V
KH 21	$Ab_{38}CC_{62}$	14.12% N.C.	5.0	1250	4	L_S + L_C + V
KH 25	$Ab_{38}CC_{62}$	9.00 % N.C.	5.1	1250	3	L_S + L_C + V
KH 27	$Ab_{25}CC_{75}$	22.54% N.C.	5.1	1250	3	L_S + L_C + V
KH 42	$Ab_{25}CC_{75}$	37.08% N.C.	5.1	1250	26	L_S + L_C + V
KH 58	$Ab_{50}NC_{50}$		5.1	1250	26	L_S + L_C + V
KH 67	$Ab_{25}CC_{75}$	10% S.O.	5.2	1225	12	L_S + L_C + V
KH 70	$An_{15}CC_{85}$		5.0	1250	12	L_S + L_C + V
KH 73	$Ab_{38}CC_{62}$	45.69% N.C.	5.0	1250	12	L_S + L_C + V
KH 77	KH11	13% S.O.	5.4	1225	19	L_S + L_C + V
KH 84	$An_{33}CC_{67}$	10% O.A.	5.1	1100	24	Gehl + L_S + L_C + V
KH 118	$Ab_{25}CC_{75}$		5.2	1125	12	L_S + L_C + V
KH 119	$E1_{25}CC_{75}$		5.	1175	12	L_S + L_C + V
KH 120	$E2_{35}CC_{65}$		5.	1175	12	L_S + L_C + V
KH 121	$E2_{35}CC_{65}$	5% O.A.	5.2	1125	12	Gehl + L_S + L_C + V

Ab: albite; An: anorthite; E1: powdered glass of composition E1; E2: powdered glass of compositon E2; CC: calcium carbonate; NC: sodium carbonate; S.O.: silver oxalate; O.A.: oxalic acid dihydrate; L_S: silicate melt; L_C: carbonate melt; V: vapour; Gehl: gehlenite crystals.

Textural features of the charges are consistent with a pair of immiscible liquids that have quenched from the P–T conditions of the run. The two phases are always separated by a sharp boundary forming a meniscus between the two liquids. In places the menisci are distorted due to several spheres coalescing (Figs. 1 and 3). The presence of coalescing spheres is another indication of the liquid state of the system before quench. The boundary between the silicate and carbonate phases is sharp to about 1 μm as evidenced by optical and electron microprobe backscattered imaging. Separation of the two liquids appears to be independent of the run duration, i.e. the physical appearance is unchanged when comparing 3- and 19-hour runs. All runs are considered to represent stable liquid immiscibility; albite–calcite and (SiO_2 + Al_2O_3 + CaO)–calcite pairs both show evidence of coalescing spheres, and the sizes of these spheres are at least one to two orders of magnitude larger than the maximum sphere size (2 μm) produced by quench (metastable) liquid immiscibility according to the data of Freestone (1978).

Vesicles were observed in all runs. The vesicles are probably the result of excess CO_2 or $CO_2 + H_2O$ which existed as a vapour at the P–T conditions of the run. All sample capsules released CO_2 or CO_2 and H_2O when opened after the run.

Analytical methods. Run products were analysed by standard microprobe techniques using a Cameca Camebax fitted with a Link Systems 860-500 E.D.S. system and ZAF4/FLS quantitative analysis software. Accelerating potential was 15 kV and specimen current *c.* 3.0 nA. A focused spot beam was rastered over an area (min. = 10 μm × 10 μm; max. = 125 μm × 125 μm) for a 100 second live count time in order to reduce volatilization of Na during the analysis. Glasses and carbonates were analysed for Si, Al, Na, Ca and Mg by E.D.S. Carbonates, which on quench had exsolved into dendritic intergrowths of calcite and nyerereite, initially presented an analytical problem. The calcite and nyerereite phases were probed independently. An average analysis of these two phases was also recorded by rastering the beam over a wider area. However, the average analysis did not lie on the tie line between the two independently analysed carbonate phases but was richer in SiO_2 and Al_2O_3. Closer inspection revealed spheres of silicate glass in the carbonate (see Fig. 2), these spheres being essentially identical to the composition of the main silicate mass. Therefore the actual composition of the carbonate liquid conjugate to the silicate liquid must lie at the intersection of the tie line between the two carbonates and the extension of the tie line from the silicate liquid to average carbonate liquid; this latter tie line passes through (or very close to) the starting bulk composition. Fig. 4 illustrates this tie line construction to deduce the carbonate liquid composition.

Achievement of equilibrium. Textural features believed to represent the presence of two liquids have been outlined previously in this paper. Chemical equilibrium is generally believed to have been achieved because: (1) silicate glasses were compositionally homogeneous as determined by microprobe; (2) various sizes of silicate glass spheres in the quench carbonate melt had compositions which compared well with the main mass of silicate glass; (3) carbonate melts were of homogeneous composition, and in carbonates that had exsolved into two phases, dendritic carbonate intergrowths of calcite and nyerereite, the 'average' analysed composition of the two carbonates

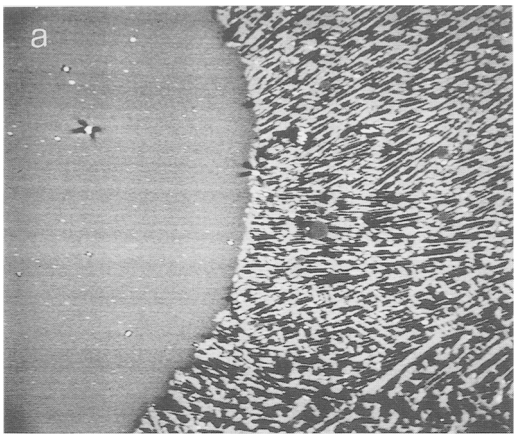

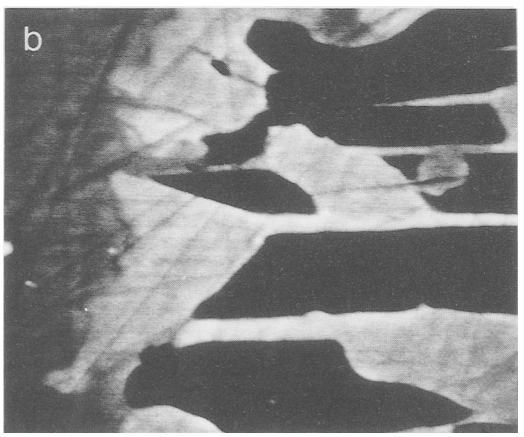

FIG. 2. BSE images. Run KH 27, $Ab_{25}CC_{75}$ plus 22.5% NC at 5 kbar and 1250 °C. (*a*) Mass of silicate, light grey (left), showing meniscus against the quench carbonate (right). The quenched carbonate liquid is an intergrowth of nyerereite (black) and calcite (white). Note numerous, small (30–100 μm) silicate spheres (light grey) within the quench carbonate. Field of view is about 3000 μm wide. (*b*) Higher magnification of (*a*) showing the meniscus and nyerereite/calcite intergrowth. Photograph is about 50 μm wide.

was constant; (4) various sizes of carbonate spheres in the main silicate mass had compositions which compared well with that for the main carbonate mass; (5) tie lines between silicate and carbonate liquids passed through or close to the starting bulk composition; (6) two liquid compositions of 3-hour runs were essentially the same as the two liquid compositions of 12- or 19-hour runs using the same P–T conditions and starting bulk compositions.

Results

Tables 2, 3 and 4 show the results from the critical runs which form the basis of this paper and the data

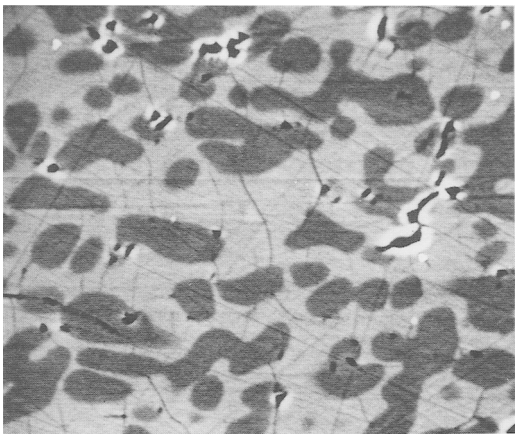

FIG. 3. BSE image. Run KH 118 $Ab_{25}CC_{75}$ at 5 kbar and 1125 °C. Host of quenched silicate melt (light grey) with coalescing carbonate droplets (dark grey). Spheres range in size from 8 to 30 μm.

are shown graphically on the $(SiO_2+Al_2O_3)$–Na_2O–CaO triangular plot (Fig. 5) after Freestone and Hamilton (1980). The pressures for all of the runs are within the range 4.9 to 5.2 kbar so that Fig. 5 can be considered to be essentially isobaric. Most of the data actually used to fix the two limbs of the immiscibility zone are for 1250 °C so that the

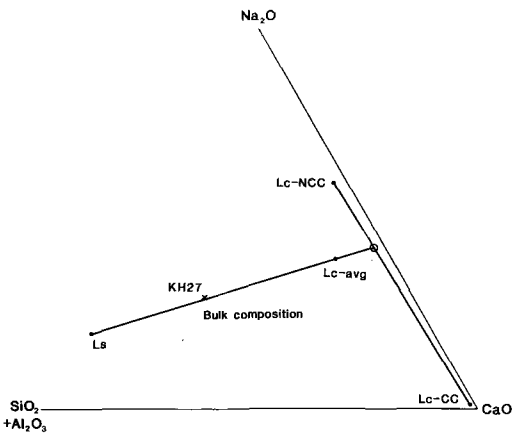

FIG. 4. Graphical construction used to determine the composition of the carbonate liquid using probe data; see text for detail. L_c–NCC = Na_2O and CaO-rich member of the intergrowth. L_c–CC = CaO-rich member of the intergrowth. L_c–avg. = composition of total carbonate intergrowth which will include a few silicate spheres and which was determined on a large area of the quenched carbonate liquid. L_s = composition of the quenched silicate liquid. Weight per cent.

Table 3 Microprobe Data. Analyses of quenched liquid phases from experimental runs. Energy dispersive techniques were used.

Run No.	Phase	SiO_2	Al_2O_3	Na_2O	CaO	MgO	Total
KH 9	L_S	41.43	11.78	6.91	33.46	-	93.58
KH 10	L_S	35.52	9.76	6.72	40.32	-	93.32
	L_C	1.35	.36	.74	55.38	-	57.83
KH 11	L_S	32.38	8.62	6.22	42.92	-	90.14
	L_C	1.60	.36	.28	55.46	-	57.70
KH 16	L_S	50.79	14.47	18.04	13.57	-	96.87
KH 21	L_S	44.16	11.25	12.26	23.16	-	90.83
	L_C-avg	6.09	.49	14.33	40.78	-	61.69
	L_C-cc	1.82	.09	.65	53.71	-	56.27
	L_C-NCC	2.17	.21	28.28	28.49	-	59.14
KH 25	L_S	39.01	10.70	11.05	28.67	-	89.43
	L_C-avg	10.38	1.41	9.63	42.03	-	63.45
	L_C-cc	.49	.22	.23	55.67	-	56.61
	L_C-NCC	2.40	.25	22.02	31.23	-	55.90
KH 27	L_S	46.88	11.54	14.87	19.35	-	92.64
	L_C-avg	6.24	.60	19.89	36.49	-	63.22
	L_C-cc	.49	.10	.22	59.94	-	55.75
	L_C-NCC	1.33	.11	28.16	29.40	-	59.00
KH 42	L_S	45.10	17.91	17.58	14.40	-	94.99
	L_C-avg	5.16	.77	24.56	29.15	-	59.64
	L_C-cc	.44	.02	.29	55.30	-	56.05
	L_C-NCC	.87	.14	28.58	28.22	-	57.81
KH 58	L_S	53.35	15.68	25.47	ø	-	94.50
	L_C	.31	.31	52.73	ø	-	53.35
KH 67	L_S	32.09	9.14	5.88	42.38	-	89.62
	L_C	1.05	.19	.16	55.83	-	57.23
KH 70	L_S	26.93	27.22	-	42.46	-	96.61
	L_C	.36	.20	-	54.43	-	54.99
KH 73	L_S	50.94	17.56	21.60	7.20	-	97.30
	L_C	1.14	.26	32.64	22.16	-	56.20
KH 77	L_S	32.14	8.84	6.13	42.04	-	89.15
	L_C	.61	.07	.11	56.00	-	56.79
KH 84	L_S	30.94	18.47	-	38.29	-	87.70
	G	23.55	35.46	-	40.09	-	99.10
	L_C	.27	.03	-	54.77	-	55.07
KH 118	L_S	34.48	9.67	6.34	43.45	-	93.94
	L_C	.96	.26	.03	58.04	-	59.29
KH 119	L_S	36.05	9.90	-	48.44	-	94.39
	L_C	.34	.04	-	56.51	-	56.89
KH 120	L_S	34.48	17.91	-	91.74	2.26	94.13
	L_C	.38	.18	-	54.83	.11	55.541
KH 121	L_S	34.99	16.62	-	40.52	4.66	96.79
	G	23.67	35.79	-	41.14	.37	100.97
	L_C	.30	.08	-	55.52	.10	55.90

L_S: silicate melt; L_C: carbonate melt; L_C-avg; average carbonate melt, consisting of three phases (see text); L_C-cc: calcium carbonate phase from L_C-avg; Lc-NCC: sodium calcium carbonate phase from L_C-avg; G: gehlenite crystals.

diagram is also isothermal, although a few results from lower-temperature runs are included for comparative purposes. On Fig. 5 the starting or bulk composition for each run is shown by a cross with the run number nearby. For example Run KH58 started with a mixture of albite glass and Na_2CO_3 (Ab, NC). After the run the charge consisted of two quenched liquids, as shown in Fig. 1. Each quenched liquid was analysed on the probe and the two compositions are shown as triangles in Fig. 5; the triangles are shown connected by a compatible join. Runs KH73, 42, 27, 21, 25, were all mixtures of

Table 4 Na_2O/CaO ratio versus $SiO_2 + Al_2O_3$ for the silicate melt fraction, bulk composition, and carbonate melt fraction in seven experimental runs

	Silicate		Bulk		Carbonate	
	Na_2O/CaO	$SiO_2 + Al_2O_3$	Na_2O/CaO	$SiO_2 + Al_2O_3$	Na_2O/CaO	$SiO_2 + Al_2O_3$
KH 10	.167	49.05	.133	47.77	.013	3.00
KH 11	.125	45.49	.070	32.90	.005	3.40
KH 21	.529	61.11	.414	40.37	.390	3.65
KH 25	.430	58.94	.300	42.67	.204	1.75
KH 27	.768	63.06	.635	39.50	.531	2.00
KH 92	1.214	66.27	.891	21.73	.824	1.60
KH 73	2.999	70.41	1.55	27.48	1.473	2.49

albite glass with calcite (CC) plus a varying proportion of NC; their bulk and run product compositions are shown on Fig. 5 by crosses and triangles respectively. The two compositions KH10 and 11 were both mixtures of albite glass and CC to which silver oxalate had been added to produce excess CO_2; the addition of silver oxalate proved to have no effect on the result of the experiment so that in subsequent runs it was not used. The products of all these runs contained two quenched liquids as shown in Fig. 5. Table 4 illustrates that, in all runs, CaO is enriched into the carbonate liquid and Na_2O into the silicate liquid. The carbonate-rich liquid compositions have been joined and represent one limb of the immiscibility solvus. The silicate liquid compositions have similarly been joined to give the silicate limb of the solvus; this latter has been extended to the Na_2O-free base of the triangle by a dashed line as shown on Fig. 5 and the rationale for doing this is discussed below.

The alkali-free base line

The starting silicate material for all the runs within the triangle was albite glass and the obvious choice for a Na_2O-free compositions was anorthite. We have done a number of runs using anorthite + calcite ± oxalic acid dihydrate ± silver oxalate, but for brevity only two are described in Fig. 5 and in Table 2, viz. KH70 and KH84. Liquid immiscibility was achieved in the run products of KH70 (5 kbar, 1250 °C) in which the carbonate composition was essentially 100% $CaCO_3$, and the silicate liquid composition is shown at the point marked 70 on the figure which is much richer in $SiO_2 + Al_2O_3$ than the dashed line extension of the silicate limb of the solvus. Either the silicate limb bends acutely between liquids KH10 and KH70 or there is some inconsistency between the two sets of data, one for albite-based runs and one for the albite-free anorthite-based runs.

One possible explanation is that the very different Al/Si ratios of the two host silicate melts is having a large effect on the silicate/carbonate immiscibility gap because of the differences in the silicate melt structures. To test this assumption composition EI (a eutectic composition in the SiO_2-Al_2O_3-CaO system) with a ratio of SiO_2/Al_2O_3 much closer to albite than the anorthite starting material, was made up and used in KH119 (run at 5 kbar and 1175 °C). The composition of the quenched silicate melt of this run (dot marked 119 on Fig. 5) is nearer to the dashed line extension of the immiscibility boundary than K70 but plots only about midway between the two. The temperature of KH119 was 1175° compared to 1250 °C for the runs used to construct the trace of the field boundary, but the temperature effect on the silicate liquid composition in the series KH11 (1250°), KH67 (1225°) and KH119 (1125°) (see Table 2) is quite small and not enough to account for the displacement of KH 119 liquid composition to lower CaO values compared with the extrapolated field boundary. Clearly the extent of the miscibility gap depends not only on P and T but also on the silicate melt composition. Not only are our data too few to draw any conclusions but also the Freestone and Hamilton plot is inadequate to show the effect of subtle changes of composition on the extent of immiscibility.

A few runs on the MgO-bearing composition E2 are included on Fig. 5 and in Table 2, as well as a few lower temperature runs. These latter had euhedral crystals of gehlenite in the run products whose composition, determined by the probe, is shown on Fig. 5.

Previous experimental work

Watkinson and Wyllie have worked on two joins which are very relevant to the subject of this paper. One of these, published in 1971, determined the phase relations along the join $NaAlSiO_4$-$CaCO_3$ with 25% H_2O at 1 kbar. This join is shown on our Fig. 6 marked Ne-CC and it cuts across our two-liquid field, but since Watkinson and Wyllie did not observe any liquid immiscibility, the two sets of data are in conflict. We have no certain

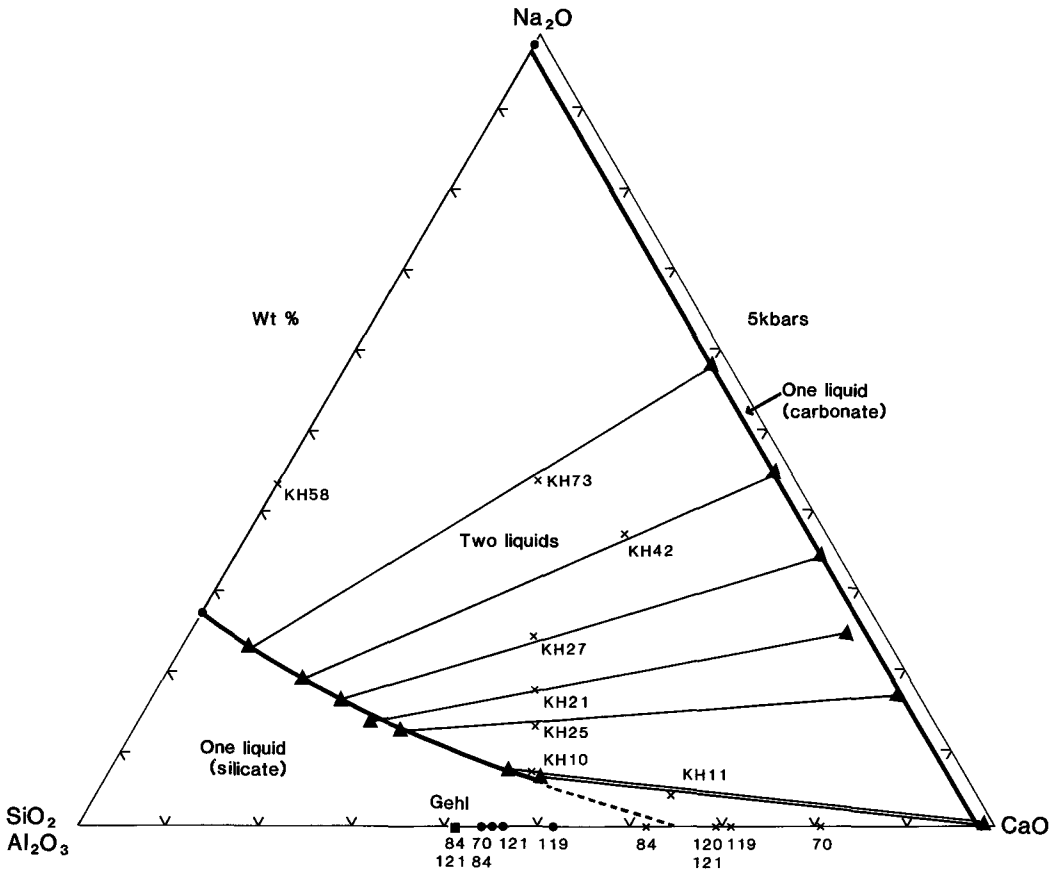

FIG. 5. The experimentally determined two-liquid field at 5 kbar and 1250 °C for Na_2O-bearing compositions. The crosses mark the starting composition and the run members are also shown. A number of Na_2O-free starting compositions and their subsequent silicate-rich melt composition formed at 5 kbar and in the temperature range 1100 to 1250 °C are shown on the base line; the significance of these is discussed in the text. GEHL is the composition of gehlenite crystals observed in some Na_2O-free runs. Weight per cent.

answer to this discrepancy but there are several possibilities: (*a*) Freestone and Hamilton (1980) have shown that immiscibility is enhanced by increasing pressure; perhaps the two-liquid field at 1 kbar has contracted to the area above the nepheline-calcite join compared to our 5 kbar diagram; (*b*) the effect of 25% H_2O has destroyed the immiscibility; (*c*) perhaps the two-liquid structure in their runs was present but so fine-grained as to be undetectable; certainly we found the back-scattered electron image invaluable in recognizing immiscibility textures. In an earlier paper, Watkinson and Wyllie (1969) published the relations in the albite-calcite plus 25% H_2O system at 1 kbar. Unfortunately, due to temperature limitations of their equipment, the join was studied only between albite and albite 60%, calcite 40%; this line is shown on our Fig. 6 as Ab–CC and can be seen to stop short of our two-liquid field.

Verwoerd (1978) has published the compositions of coexisting silicate and carbonate melts at 2 kbar and 900 °C. His starting material was a mixture of 30% synthetic ijolite, 70% synthetic natrocarbonate. These liquid compositions are shown on our Fig. 6 as line 9 and the slope of his tie-line is in excellent agreement with our data.

Brey and Green (1976) melted an olivine melilitite at $P > 20$ kbar and reported possible liquid immiscibility textures. Brey (1977) added calcic dolomite to the melilitite but failed to enhance the two-liquid texture. The composition of their rock plots at the left end of the line marked

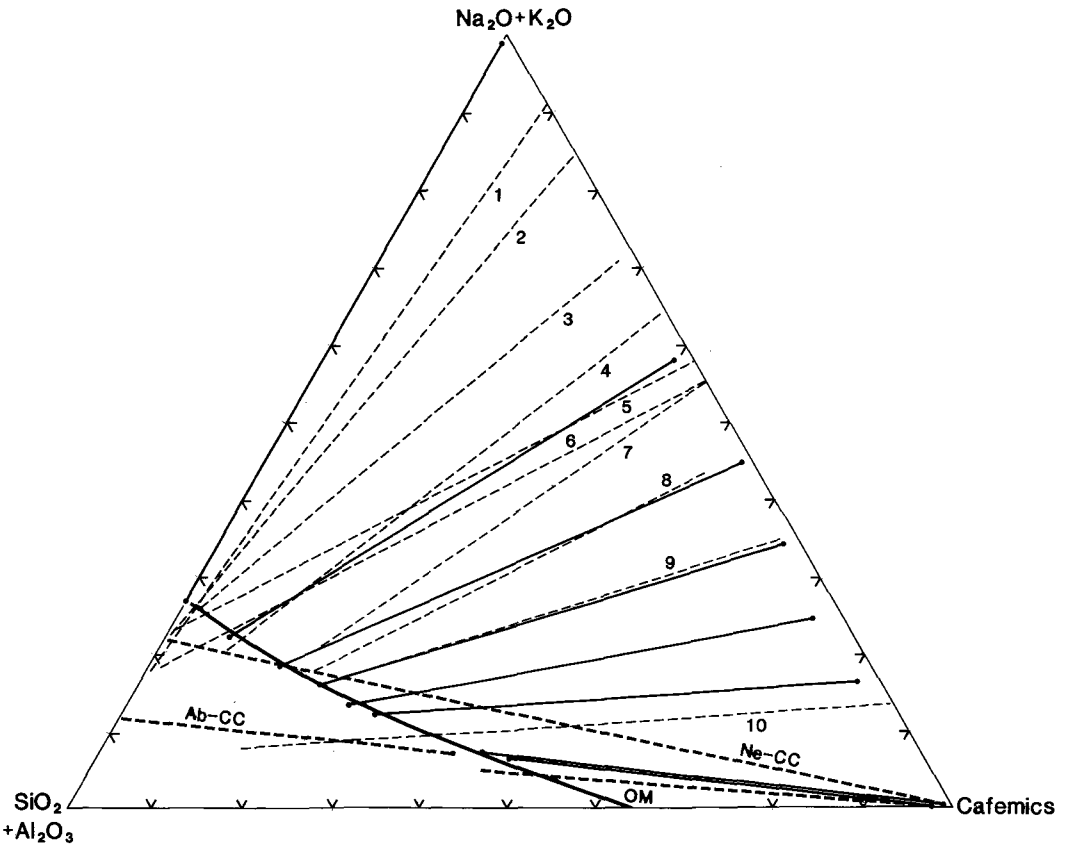

FIG. 6. Compilation of experimental data from several sources relevant to carbonate–silicate liquid immiscibility. The heavy line across the SW corner is the trace of the silicate limb of the immiscibility dome determined at 5 kbar and 1250 °C (this study). There are seven liquid–liquid tie lines shown as full lines with dots marking the liquid compositions at either end (data from this study). Dashed lines numbered 1, 2, 5, 6 are tie lines from Koster van Groos and Wyllie (1973), dashed tie lines 3, 4, 7 are from Freestone and Hamilton (1980), 8 is from Bedson (1983), 9 from Verwoerd (1978) and 10 is from Koster van Groos (1975). The heavy dashed line marked OM is the olivine–melilite–dolomite join worked on by Brey and Green (1976); the one labelled Ab–CC is the albite–calcite join worked on by Watkinson and Wyllie (1969); Ne–CC is the nepheline–calcite join of Watkinson and Wyllie (1971). No immiscibility was found by the original workers on these latter two joins. Weight per cent.

OM on our Fig. 6 and their added carbonate will plot at the cafemic corner. According to our results their mixture should have shown immiscibility, but the effect of pressure on the two-liquid field much above 8 kbar is not known and is certainly worthy of study.

Petrology

Immiscibility between silicate and carbonate melts has been demonstrated in the laboratory by many workers; this paper shows for the first time that carbonate melts of almost 100% $CaCO_3$ are immiscible with some silicate melts which themselves are very poor in $K_2O + Na_2O$. These new data should have some impact on theories on the genesis of carbonatites. We propose to discuss a few ideas here under two headings; (i) carbonate ocelli found in basic dyke rocks, (ii) the much larger carbonatite masses found with alkali-rich silicate rocks in ring complexes.

(i) *Carbonate ocelli.* There are a few examples of these described in the literature, e.g. Seabourn Lake, Canada (Ferguson and Curry, 1971); the Benfontein Sill, R.S.A. (Dawson and Hawthorne, 1973); Sinai (Bogoch and Magaritz, 1983); Spitsbergen (Amundsen, 1987) but the list is growing. The simplest explanation for the origin of these

round blobs of carbonate in a basic igneous rock is droplets of one liquid within another. The compositions of the carbonate ocelli are invariably alkali-free, consisting of $CaCO_3 + MgCO_3$ with small amounts of Fe, P, Mn, etc. and experimental work did not offer support for immiscibility being possible with these compositions. The new data of the present paper demonstrate the existence of immiscibility in very similar synthetic compositions and should now allow the obvious conclusion to be drawn that ocellar structure represents frozen two-liquid equilibrium. There must also be natural systems where the carbonate droplets have coalesced to form layers (we may have evidence of this process in the Benfontein sill) and eventually to form a separate magma; the well-known Premier Mine carbonate sill cutting kimberlite is a possible example of this.

If there has been little or no movement of the silicate magma after the immiscibility event the carbonate droplets will remain spherical, but movement might modify them so that a range of shapes of isolated carbonate material could result. It should be noted here that no alkali metasomatism associated with this class of carbonatites would be expected because very little if any Na_2O and K_2O would be in the system. Carbonate very rich in Ca and Mg will be relatively refractory but the small amounts of Fe, P, H_2O, etc., that are invariably present will almost certainly lower the liquidus temperatures to those expected in the basic to ultrabasic silicate melt fraction of the system,

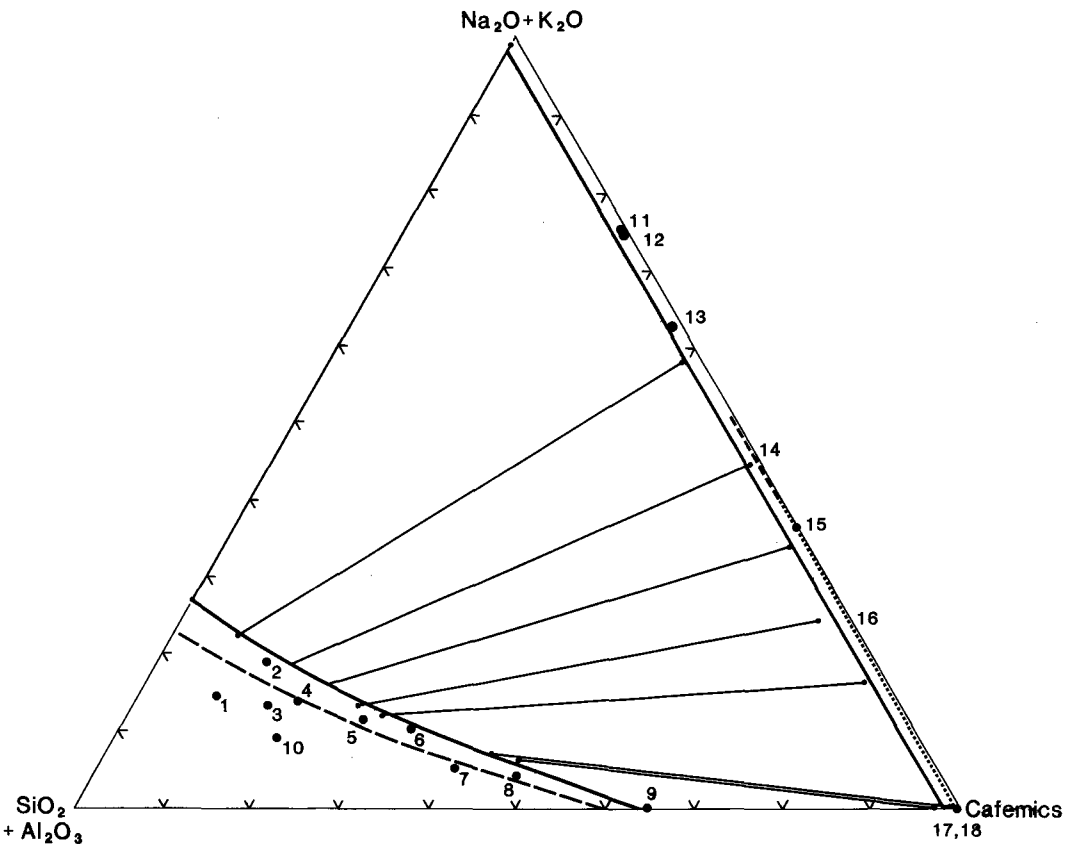

FIG. 7. Plot of natural compositions compared to the trace of immiscibility dome for 5 kbar. The seven straight lines join conjugate silicate–carbonate conjugate liquids as determined in this study: 1 = phonolite; 2 = urtite; 3 = nepheline syenite; 4 = nephelinite; 5 = micro-ijolite; 6 = ijolite; 7 = melanephelinite; 8 = melilitite (all found in carbonatite complexes and taken from Le Bas, 1977); 9 = kimberlite from the Benfontein sill (Dawson and Hawthorn, 1973); 10 = lamproite, Vera (Borley, 1967); 11 and 12 = natrocarbonatites, Oldoinyo Lengai (Dawson, 1962); 13 = carbonate in liquid inclusion (Aspden, 1977); 14 = calcified natrocarbonate tuff (Deans and Roberts, 1984); 15 and 16 = carbonate inclusions in apatite (Aspden, 1981 and 1977); 17 = carbonate in Benfontein sill (Dawson and Hawthorn 1973).

i.e. 1050–1200 °C. Carbonate groundmass veins, stringers, dykes, etc., are often reported in association with kimberlites and lamproites. These are often described as secondary material not associated with the solidification of the main silicate rock, but in our opinion some of these carbonates could probably represent conjugate liquids with the kimberlite or lamproite melt. Further, at least some of the carbonate material often found with dolerite dykes might also be carbonatite exsolved from the parent silicate magma.

(ii) *Carbonatites in ring complexes.* This field association has been described in detail by many writers. Our ideas on the role of immiscibility in the generation of the wide range of both silicate and carbonatite rocks found in these complexes are set out below. Our starting point is a mantle-derived alkali-rich and carbonated basic silicate magma which is moving upwards and is undergoing fractional crystallisation due to falling temperature. At some stage the melt phase of this magma will reach a critical level of carbonate concentration and droplets of a carbonatite magma will be exsolved. The most primitive silicate rock found in the ring complexes seems to be a melilitite and this composition seems a likely candidate for the magma composition close to the stage of the initial immiscibility. To be better able to plot rock compositions on the triangle of Fig. 6 we have increased the number of components in the bottom right corner from CaO to CaO + MgO + FeO + Fe_2O_3 and labelled this corner Cafemics in Fig. 7. We have also shown on Fig. 7 the two limbs of the immiscibility solvus for 5 kbar and an additional silicate limb for 8 kbar (shown as a dashed line). This latter line has been drawn parallel to the 5 kbar solvus and its position has been estimated from the higher-pressure results of Freestone and Hamilton (1980). Also on Fig. 7 are conjugation lines joining two liquid compositions in equilibrium at 5 kbar and 1250°, these are taken from Fig. 6. We have plotted on Fig. 7 a number of silicate rock compositions most of which are taken from Le Bas (1977) (see legend and Table 5). A typical melilitite found in association with carbonatites plots at point 8 on Fig. 7 and can be seen to have as a conjugate liquid a carbonate plotting very close to the Cafemic corner, i.e. very poor in K + Na, but rich in Ca, Mg, Fe, Mn. The actual ratio of the latter elements will depend on *PTX*; our data, so far, are too scanty to make accurate predictions. Many, but not all, carbonatites have abundances of rare earth and other incompatible elements which can be up to several orders of magnitude greater than in the associated silicate rocks. Hamilton *et al.* (1988) have shown that to get distribution coefficients of this magnitude between silicate and carbonate conjugate liquids, pressures of at least 6 kbar are required. Thus we propose that the first carbonatite liquid is exsolved at depths of 20 km or greater. Immiscibility at higher levels should lead to barren carbonatite. The carbonate melt at this stage must contain, in solution, all the elements for any potential minerals such as magnetite, apatite, baryte, Fe/Cu sulphides, baddeleyite (ZrO_2), *REE* minerals such as bastnäsite, pyrochlore, etc., because the low density and low viscosity of the carbonate melt make it incapable of transporting

Table 5. Analyses of natural silicate rocks and carbonatites

	SiO_2	Al_2O_3	TiO_2	Fe_2O_3	FeO	MnO	MgO	CaO	K_2O	Na_2O	P_2O_5	CO_2	H_2O
1	52.99	19.88	0.50	3.36	1.43	0.19	0.43	2.75	5.25	8.75	0.10	0.41	4.17
2	40.40	26.29	0.25	1.97	0.68	0.09	0.62	8.47	12.80	5.42	0.70	0.44	1.28
3	51.16	17.80	0.56	4.88	2.43	0.25	0.90	5.69	6.04	6.95	0.22	0.97	2.00
4	47.01	17.53	1.22	4.80	2.80	0.24	1.65	6.91	4.36	8.68	0.36	0.69	3.66
5	42.66	16.58	1.52	6.45	3.49	0.25	2.85	11.53	3.03	8.09	0.65	0.81	1.94
6	40.01	15.25	2.38	6.61	3.39	0.16	3.50	16.36	3.10	7.10	0.88	0.56	0.71
7	41.52	10.78	2.98	7.95	6.11	0.23	7.53	13.74	1.73	3.28	0.73	0.09	3.16
8	36.73	7.80	3.51	6.51	6.69	0.22	9.28	18.19	1.79	2.29	1.13	-	4.35
9	53.96	11.30	1.30	0.73	3.52	0.07	8.61	3.67	3.50	3.10	0.55	-	5.27
10	25.19	2.87	1.89	3.72	6.72	0.22	29.69	13.59	0.15	0.01	2.20	12.83	1.15
11	-	0.08	0.10	0.26	-	0.04	0.49	12.74	7.58	29.53	0.83	31.75	8.59
12	-	0.09	0.08	0.32	-	0.24	0.41	12.82	6.58	29.70	1.06	32.40	8.27
13	2.10	1.00	-	-	0.90	-	-	19.80	6.10	26.30	-	29.2	-
17	0.52	0.48	0.10	1.30	0.61	0.19	8.87	44.07	-	0.41	1.42	41.24	0.39

1) Phonolite - mean from 55 analyses (Le Bas 1977)
2) Urtite - average of 3 analyses (Le Bas 1977)
3) Nepheline Syenite - mean from 11 analyses (Le Bas 1977)
4) Nephelinite - mean from 14 analyses (Le Bas 1977)
5) Micro-ijolite - mean from 7 analyses (Le Bas 1977)
6) Ijolite - mean from 41 analyses (Le Bas 1977)
7) Melanephelinite - mean from 43 analyses (Le Bas 1977)
8) Melilitite - mean from 6 analyses (Le Bas 1977)
9) Kimberlite, Benfontein Sill (Dawson & Hawthorne 1973)
10) Verite, Vera, Spain, Sample VI of Borley (1967)
11) Oldoinyo Lengai - Dawson 1962
12) Oldoinyo Lengai - Dawson 1962
13) Le Bas 1981, Table IV, Carbonate inclusion in apatite crystal
17) Calcite rich layer BD 1048, Lower Sill, Benfontein (Dawson & Hawthorne 1973)

any heavy minerals in anything but turbulent flow conditions. The change in the composition of both melts from now on will be governed by a number of factors not least being the rate of mutual separation of the two liquids of which we know nothing. In general terms, with falling temperature, each melt will undergo both fractional crystallization and liquid fractionation (Le Bas, 1987); evidence from rock compositions (Table 5) suggests that the silicate melt will move along the limb of the solvus shown on Fig. 7 moving from point 8 (melilitite) to 7 (melanephelinite) to 6 (ijolite) to 4 (nephelinite) to 2 (urtite) to 1 (phonolite). The composition of the carbonate melt being exsolved from the silicate melt will change along the carbonate limb of the solvus of Fig. 7 becoming enriched in alkalis; when the host silicate magma is phonolite the carbonate melt will have a composition similar to the natrocarbonate of Oldoinyo Lengai, i.e. line 4 on Fig. 6 or points 11 and 12 on Fig. 7.

Carbonatite melt that moves away from the parent silicate melt will probably give rise to very different daughter melts. The main controlling factor will be fractional crystallization and the most abundant crystal phase should be calcite. Depending on initial composition p_{O_2}, etc., the residual

Sample#	%CC ppt	% F_L R
KH11	99	1
KH25	61	39
KH21	45	55
KH27	26	74
KH42	2	98

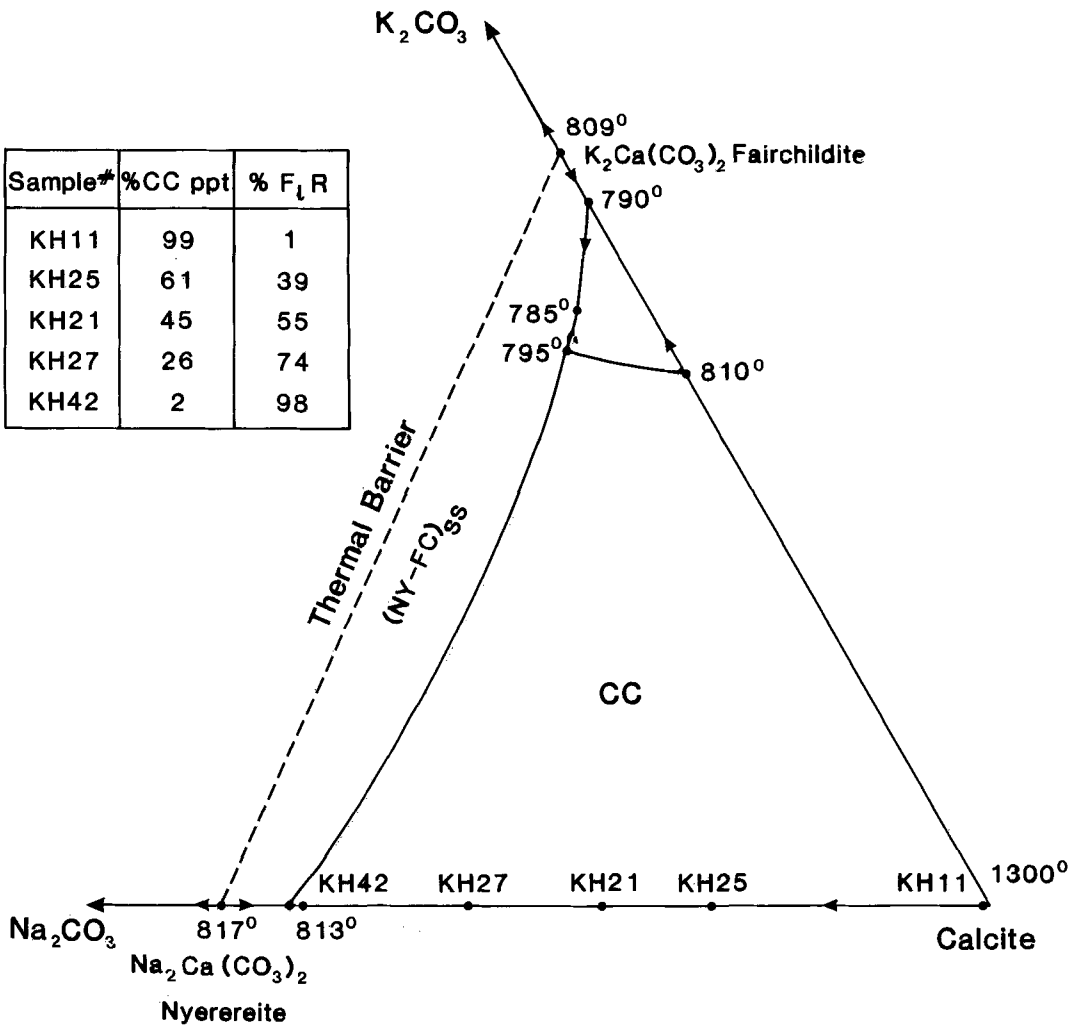

FIG. 8. Part of the Na_2CO_3–K_2CO_3–CaO_3 liquidus diagram of Cooper *et al.* (1975) on which a number of liquid compositions from this study have been plotted. The table shows the amount of calcite precipitated by each liquid before the liquid reaches the field boundary.

liquid may become enriched in alkalis, or Fe or Mg, or incompatible elements and it is this line of descent that is probably responsible for the origin of carbonatites of unusual or extreme composition, e.g. the ferrocarbonatites. Several other authors have previously arrived at this conclusion, e.g. Woolley (1982). It seems possible that this line of descent could also produce the Oldoinyo Lengai natro-carbonatites, so it seems possible to produce these Na-rich liquids by more than one process. The crystal fraction in this fractionation process, mainly of calcite (or dolomite), together with other minerals such as magnetite, apatite, sulphides, pyrochlore, etc., which have been precipitated by the carbonatite liquid and then accumulated on the floor of the magma chambers are the raw material for the coarse-grained intrusive carbonatites which ultimately form the cores of many ring complexes. The liquidus phase diagram of Cooper *et al.* (1975) is relevant to this process of accumulation of calcite; part of this diagram is shown on Fig. 8. Five of our experimentally produced carbonatite liquid compositions are plotted on this diagram: KH11, 25, 21, 27 and 42. These are conjugate to melts equivalent to a melilitite, an ijolite, a micro-ijolite, a nephelinite and an urtite respectively (see Fig. 7). The Table on Fig. 8 shows that the amounts of calcite these carbonate melts could precipitate before nyerereite is co-precipitated are 99, 61, 45, 26 and 2% respectively. All this calcite is the potential material for a sövite body which could be intruded into high-level crust because of its buoyancy aided by residual alkali-rich liquid and excess CO_2. The gneissose texture of many coarse-grained carbonatites have led field geologists to the conclusion that plutonic carbonatites are a result of a largely solid-state injection so that this idea is an old one, e.g. see Bailey (1966) for a detailed discussion. We wish merely to support this hypothesis of solid-state injection of the calcite-rich or dolomite-rich plutonic masses, even though we have demonstrated the immiscible nature of melts approximating melilitite and sövite in composition. Our results show, however, that carbonatite melts containing large amounts of potential sövite can be generated by immiscibility.

There are many outstanding problems to be solved, not least of which are the effects of P_2O_5, H_2O and F on the nature of the immiscibility gap and the behaviour of the carbonate melt after its separation from the host silicate melt. Magnetite is a ubiquitous mineral in carbonatites but its relationship to the ferrocarbonatites is unknown.

Acknowledgements

We thank Tim Hopkins and Dave Plant for their usual cheerful assistance on the microprobe, Prof. W. S. MacKenzie for helpful suggestions on the manuscript and to NERC for continued financial support to the Experimental Petrology Laboratory. B. K. would like to acknowledge a Research Scholarship from Manchester University which enabled him to work in Manchester. The manuscript was improved by the comments of the reviewers Mike Le Bas and Alan Woolley.

References

Aspden, J. A. (1977) Ph.D. thesis, University of Leicester.
——(1981) *Mineral. Mag.* **44,** 201–4.
Amundsen, H. E. F. (1987) *Nature* **327,** 692–5.
Bailey, D. K. (1966) In *Carbonatites* (O. F. Tuttle and J. Gittins, eds.) Wiley, 127–54.
Bedson, P. (1983) *The Origin Of The Carbonatites And Their Relations To Other Rocks By Liquid Immiscibility.* Ph.D. thesis, University of Manchester.
Bogoch, R., and Magaritz, M. (1983) *Contrib. Mineral. Petrol.* **83,** 227–30.
Borley, G. D. (1967) *Mineral. Mag.* **36,** 364–79.
Brey, G. (1977) IASPEI/IAVCEI Joint Assemblies, Durham, abstracts, 221.
——Green, D. H. (1976) *Contrib. Mineral. Petrol.* **55,** 217–30.
Cooper, A. F., Gittins, J., and Tuttle, O. F. (1975) *Am. J. Sci.* **275,** 534–60.
Dawson, J. B. (1962) *Bull. Volcanol.* **24,** 349–88.
——(1966) In *Carbonatites* (O. F. Tuttle and J. Gittins, eds.) Wiley 155–68.
——and Hawthorne, J. B. (1973) *J. Geol. Soc. London* **129,** 61–85.
Deans, T., and Roberts, B. (1984) Ibid. **141,** 563–580.
Eggler, D. H. (1975) *Trans. Am. geophys. Union (EOS)* **56,** 470.
Ferguson, J., and Currie, K. L. (1971) *J. Petrol.* **12,** 561–85.
Freestone, I. C. (1978) *Chem. Soc.* **23,** 115–23.
——and Hamilton, D. L. (1980) *Contrib. Mineral. Petrol.* **73,** 105–17.
Hamilton, D. L., Bedson, P., and Esson, J. (1988) Submitted chapter in book edited by K. Bell.
Holmes, A. (1952) *Trans. Geol. Soc. Edinburgh* **15,** 187–213.
King, B. C. (1949) *Geol. Surv. of Uganda Mem.* 5.
——(1965) *J. Petrol.* **6,** 67–100.
——and Sutherland, D. S. (1960) *Sci. Prog.* **48,** 298–321, 504–24, 709–20.
Koster Van Groos, A. F. (1975) *Am. J. Sci.* **275,** 163–85.
——and Wyllie, P. J. (1966) Ibid. **264,** 234–55.
————(1968) Ibid. **266,** 932–67.
————(1973) Ibid. **273,** 465–87.
Le Bas, M. J. (1977) *Carbonatite–Nephelinite Volcanism.* Wiley, 263–93.
——(1981) *Mineral. Mag.* **44,** 133–40.
——(1987) *Geol. Soc. Special Pub.* No. 30.
Middlemost, E. A. K. (1974) *Lithos* **7,** 275–8.
Verwoerd, W. J. (1978) *Carnegie Inst. Washington Yearb.* **77,** 767–74.
von Eckermann, H. (1948) *Internat. Geol. Congr.* **18**(3), 90–3.
——(1961) *Bull. Geol. Inst. Uppsala* **40,** 25–36.

——(1966) In *Carbonatites* (O. F. Tuttle and J. Gittins, eds.) Wiley, 3–31.
Watkinson, D. H., and Wyllie, P. J. (1969) *U.S. Geol. Surv. Bull.* **80,** 1565–76.
——(1971) *J. Petrol.* **12,** 357–78.
Wendlandt, R. F., and Harrison, W. J. (1979) *Contrib. Mineral. Petrol.* **69,** 409–19.
Woolley, A. R. (1982) *Mineral. Mag.* **46,** 13–17.
Wyllie, P. J. (1987) In *Magmatic Processes: Physicochemical Principles* (B. O. Mysen, ed.) The Geochemical Soc., 107–20.

[*Revised manuscript received 20 August 1987*]